Am J Transl Res 2025;17(7):5320-5331
www.ajtr.org /ISSN:1943-8141/AJTR0165018

Original Article

Serum miR-146a as a diagnostic and predictive biomarker for osteoporosis and bisphosphonate treatment efficacy

Qing Yin[1*], Rui Yang[2*], Haibo Yu[1]

[1]Department of Orthopedics, Dianjiang Traditional Chinese Medicine Hospital, Chongqing 408300, China; [2]Department of Orthopedics, Affiliated Traditional Chinese Medicine Hospital of Chongqing Three Gorges Medical College, Chongqing 404100, China. [*]Co-first authors.

Received April 2, 2025; Accepted June 24, 2025; Epub July 15, 2025; Published July 30, 2025

Abstract: Objective: To evaluate the diagnostic and predictive value of miR-146a for osteoporosis and bisphosphonate treatment outcomes, and to investigate the underlying mechanism by which bisphosphonates exert therapeutic effects via miR-146a regulation. Methods: A retrospective cohort of 96 patients with osteoporosis and 90 healthy individuals undergoing routine health examinations was analyzed. Serum miR-146a levels were measured to assess their diagnostic utility for osteoporosis. Changes in miR-146a levels before and after one year of bisphosphonate treatment and their correlation with treatment efficacy were also analyzed. In addition, in vitro experiments were conducted to examine the effects of miR-146a and bisphosphonates on osteoclast differentiation and function. Results: Serum miR-146a levels were significantly lower in osteoporosis patients and negatively correlated with disease severity, demonstrating strong diagnostic performance (AUC=0.910, sensitivity =97.78%; specificity =77.08%). Following bisphosphonate treatment, miR-146a levels increased significantly and were positively associated with treatment response, showing moderate predictive value (AUC=0.761; sensitivity =82.29%, specificity =60.42%). Bisphosphonates inhibited osteoclast differentiation, an effect reversed by miR-146a inhibition and enhanced by miR-146a overexpression. Conclusion: Serum miR-146a shows promise as a diagnostic and predictive biomarker for osteoporosis and the efficacy of bisphosphonate therapy. It plays a role in suppressing osteoclast differentiation, and bisphosphonates may exert their therapeutic effects in part by upregulating miR-146a. These findings suggest that targeting miR-146a could be a novel strategy for osteoporosis management.

Keywords: Osteoporosis, miR-146a, bisphosphonate, osteoclast, diagnostic and predictive biomarker

Introduction

Osteoporosis is a globally prevalent metabolic bone disease, predominantly affecting older adults. It is characterized by reduced bone mass and deterioration of bone microarchitecture [1], typically progressing asymptomatically until presenting as fragility fractures at weight-bearing sites, such as the hip and spine, after minimal trauma [2]. These fractures place a significant economic burden on healthcare systems, particularly in aging populations where prevalence continues to rise. The underlying pathophysiology involves an imbalance in bone remodeling, with excessive osteoclastic activity driving progressive bone loss [3]. This understanding has shaped current treatment approaches, which primarily aim to inhibit bone resorption using anti-osteolytic agents [4]. Among these, bisphosphonates have become the cornerstone of therapy, effectively reducing fracture risk and slowing disease progression [5]. However, osteoporosis management remains complex, requiring individualized treatment plans that consider patient-specific factors, potential adverse effects, and long-term outcomes.

Bisphosphonates are well established as first-line pharmacological agents for osteoporosis, demonstrating significant efficacy in reducing fracture risk. However, their use is associated with notable safety concerns, including common gastrointestinal side effects and rare but

https://doi.org/10.62347/JRIQ2431

severe complications such as osteonecrosis of the jaw, esophageal irritation, and renal impairment [6]. These risks necessitate careful patient selection and close monitoring during treatment. The diagnosis and evaluation of osteoporosis rely primarily on bone mineral density (BMD) measurements using dual-energy X-ray absorptiometry, with the hip and spine serving as key assessment sites [7]. While bisphosphonate efficacy can be monitored through BMD, interpreting BMD changes during therapy requires consideration of multiple clinical factors. The American Association of Clinical Endocrinologists provides guidelines recommending serial BMD assessments every two years after treatment initiation until BMD stabilizes, followed by continued monitoring at similar or shorter intervals [8]. This protocol applies not only to bisphosphonates but also to other anti-osteoporotic agents, underscoring the chronic nature of the disease and the importance of long-term follow-up.

Recent advances in molecular biology have transformed disease diagnostics, with real-time quantitative reverse transcription polymerase chain reaction (RT-qPCR) emerging as a precise tool for nucleic acid quantification. Among various molecular targets, microRNAs (miRNAs) have attracted considerable attention in biomedical research. MiRNAs post-transcriptionally regulate gene expression through sequence-specific binding to target sites [9]. Growing evidence indicates that miRNAs play critical roles in bone biology, regulating bone development and metabolic homeostasis [10]. For example, miR-21 is significantly upregulated in the plasma of postmenopausal women with osteoporosis and inversely correlates with BMD [11]. Overexpression of miR-210 has been shown to increase BMD and ameliorate postmenopausal osteoporosis in rats by promoting vascular endothelial growth factor expression [12]. Notably, miR-146a has emerged as a key regulator, suppressing osteoblast activity and bone formation [13], suggesting its therapeutic relevance in osteoporosis. Moreover, plasma miR-146a levels are significantly reduced and associated with muscle mass loss in postmenopausal osteoporotic women [14]. Interestingly, zoledronic acid, a bisphosphonate, upregulates miR-146a levels in osteoclast-derived extracellular vesicles, thereby inhibiting osteoclast function [15]. These findings suggest that serum miR-146a may play a critical role in mediating the therapeutic effects of bisphosphonates in osteoporosis patients and holds promise as both a biomarker and a potential therapeutic target.

Materials and methods

Clinical study cohort

To ensure sufficient statistical power, the required sample size for the retrospective cohort was estimated using G*Power 3.1 based on preliminary data (expected effect size =1.5, α=0.05, power =80%), indicating that at least 84 participants per group were needed. To account for potential data variability and the exclusion of incomplete records, the study group included 96 patients diagnosed with osteoporosis who received treatment at Dianjiang Traditional Chinese Medicine Hospital between January 2023 and January 2024. For comparison, 90 healthy individuals undergoing routine health examinations during the same period were recruited as control group.

Osteoporosis was diagnosed based on BMD measurements obtained by dual-energy X-ray absorptiometry at the femoral neck or lumbar spine. Diagnostic categories were defined as follows: (1) normal bone mass: T-score ≥-1.0; (2) osteopenia (low bone mass): T-score between -1.0 and -2.5; and (3) osteoporosis: T-score ≤-2.5 or evidence of fragility fractures.

For study inclusion, osteoporosis was defined as a BMD value at least 2.5 standard deviations below the young adult female reference mean.

Rigorous exclusion criteria were applied to ensure study validity, excluding individuals with: (1) hematological disorders; (2) malignant neoplasms; (3) documented hypersensitivity to bisphosphonates; or (4) severe renal impairment. This study was reviewed and approved by the Institutional Review Board of Dianjiang Traditional Chinese Medicine Hospital.

Treatment methods

Patients in the study group were stratified into three treatment groups based on the prescribed bisphosphonate regimen: (1) risedronate group; (2) alendronate group; and (3) zole-

dronic acid group. All patients concurrently received daily calcium carbonate D_3 supplementation (Wyeth Pharmaceuticals, USA), with two tablets per dose providing a total of 1200 mg of elemental calcium and 250 IU of vitamin D, throughout the one-year treatment period.

Risedronate group: patients received 5 mg of oral risedronate sodium daily (Kunming Jida Pharmaceutical Co., Ltd.; China FDA Approval No. H20080119). They were instructed to take the tablet with 240 mL of plain water while in an upright position, 30-60 minutes before eating, and to remain upright for at least 30 minutes afterward.

Alendronate group: patients received 70 mg of oral alendronate sodium once weekly (Merck & Co., Inc., Hangzhou; China FDA Approval No. J20130085). Tablets were taken with a full glass of water before breakfast, with patients remaining upright and refraining from eating or lying down for at least 30 minutes afterward. Alendronate was contraindicated in patients with esophageal stricture or other conditions causing delayed esophageal emptying, or in those unable to sit or stand upright for at least 30 minutes.

Zoledronic acid group: patients received an intravenous infusion of zoledronic acid (Beijing Novartis Pharmaceutical Co., Ltd.; China Registration No. H20181132) at a dose of 5 mg once annually.

Efficacy assessment

Routine tests: Complete blood and urine counts; liver and kidney function tests; and measurements of serum calcium, phosphorus, and bone-specific alkaline phosphatase levels.

Bone metabolism markers: The bone resorption marker β-C-terminal telopeptide of type I collagen (β-CTX) and urinary deoxypyridinoline/creatinine ratio (DPD/Cr) were measured using electrochemiluminescence immunoassay. Tartrate-resistant acid phosphatase 5b (TRACP-5b) was quantified by enzyme-linked immunosorbent assay.

BMD evaluation: BMD of the lumbar spine (L2-L4) and unilateral hip femoral neck was measured for all patients before and one year after treatment using a Lunar Prodigy Advance PA+300164 dual-energy X-ray absorptiometry (DEXA) scanner (GE, USA). Intergroup differences were analyzed.

Evaluation of therapeutic efficacy: Markedly effective: Complete resolution of pain and increased BMD on examination. Effective: Significant pain relief with stable or increased BMD. Ineffective: No improvement in symptoms or BMD compared to baseline.

Monitoring of adverse events: Acute reactions (e.g., fever, myalgia); gastrointestinal symptoms and bowel disturbances; musculoskeletal disorders; osteonecrosis of the jaw; and atypical fractures.

RT-qPCR

Serum miR-146a levels in both groups were quantified by RT-qPCR to evaluate its diagnostic value for osteoporosis and to assess changes before and after treatment. In brief, total RNA was extracted from serum samples using TRIzol reagent (R0016; Beyotime, Shanghai, China). cDNA synthesis was performed using the PrimeScript™ II First Strand cDNA Synthesis Kit (No. 6210A, TaKaRa, Beijing, China). RT-qPCR was carried out using SYBR Green Master Mix (Applied Biosystems, USA).

Twenty μL RT-qPCR reaction mixture contained 5.0 μL of cDNA, 5.0 μL of forward primer, 5.0 μL of reverse primer, 10.0 μL of 2× SYBR Green PCR Master Mix, and 4.0 μL of ddH_2O. MiR-146a expression was normalized to U6 small nuclear RNA using the 2^-ΔΔCT method. Primers (GeneCopoeia, Guangzhou, China) were as follows: miR-146a: forward 5'-AGAACTGAATTCCATGGGTT-3', reverse 5'-GACAGAGATATCCCAGCTGAAGAA-3'. U6: forward 5'-ATTGGAACGATACAGAGAAGATT-3', reverse 5'-GGAACGCTTCACGAATTTG-3'.

Isolation and culture of bone marrow mononuclear cells (BMMCs)

Five 2-day-old Sprague-Dawley neonatal rats were obtained from Yisen Biotechnology (Shanghai, China). All animals were housed under standard laboratory conditions (22±3°C; 50±5% relative humidity). All experimental procedures were approved by the Institutional Animal Care and Use Committee of Dianjiang Traditional Chinese Medicine Hospital. Follow-

ing deep anesthesia with intraperitoneal pentobarbital sodium (50 mg/kg), rats were euthanized by cervical dislocation, and the long bones of the limbs were aseptically harvested. The bones were immediately immersed in cold D-Hank's solution containing antibiotics. Muscle and soft tissue were carefully removed, and the metaphyseal segments were excised. The bones were then placed in 5 mL of Dulbecco's Modified Eagle Medium (DMEM) supplemented with 10% fetal bovine serum (FBS) and incubated at 4°C for 30 minutes. Subsequently, the bones were cut transversely into 4-5 mm segments and longitudinally sectioned to expose the inner cortical surface. The fragments were flushed repeatedly for 5-10 minutes using a pipette, and the resulting cell suspension containing BMMCs was collected.

The suspension was transferred into a 35 mm culture dish and incubated at 37°C in a humidified atmosphere of 5% CO_2 for 10 minutes. Non-adherent cells were filtered through a 200-mesh cell strainer and centrifuged (1000 rpm, 10 minutes, 4°C). After discarding the supernatant, the pellet was resuspended and filtered again through a 200-mesh strainer to remove residual non-osteoclast cells and debris. The purified cells were seeded into culture flasks at a density of 1×10^6 cells/mL. After 12 hours, the medium was replaced to remove red blood cells and residual non-adherent cells, with subsequent medium changes every two days. BMMCs were cultured with 50 ng/mL macrophage colony-stimulating factor (M-CSF) and 50 ng/mL receptor activator of NF-κB ligand (RANKL) for five days to induce osteoclast differentiation.

Cell transfection

Differentiated osteoclasts were resuspended in fresh medium and seeded into 6-well plates at a density of 1×10^5 cells/well. When cell confluence reached 60%-70%, cells were transfected with miR-146a mimics or inhibitors using Lipofectamine 2000 reagent (11668-019; Life Technologies, Shanghai, China) according to the manufacturer's instructions. After 24 hours, total RNA was extracted. MiR-146a oligonucleotides were designed and synthesized by GenePharma (Shanghai, China).

TRAP staining

Following the indicated treatments, osteoclasts were fixed with 4% paraformaldehyde and stained for TRAP activity (Sigma-Aldrich, USA). TRAP-positive multinucleated cells (≥3 nuclei) were visualized under an inverted microscope (Olympus, Japan) at 200× magnification and quantified using ImageJ software.

Western blot analysis

Total protein was extracted using radioimmunoprecipitation assay (RIPA) buffer, separated by 10% sodium dodecyl sulfate-polyacrylamide gel electrophoresis (SDS-PAGE), and transferred to polyvinylidene fluoride (PVDF) membranes. Membranes were incubated overnight at 4°C with primary antibodies (1:1000 dilution), followed by incubation with appropriate secondary antibodies at 25°C for 2 hours. Protein bands were visualized by enhanced chemiluminescence and quantified using ImageJ software. Primary antibodies were purchased from Abcam: TRAP (ab151239), cathepsin K (CTSK; ab19027), and glyceraldehyde-3-phosphate dehydrogenase (GAPDH; ab9485).

Statistical analysis

Data analyses were performed using SPSS 19.0. Categorical data were expressed as rates and compared using the χ^2 test. Continuous data were presented as mean ± standard deviation (SD) and analyzed using Student's t-test. Correlations were assessed by Spearman's or Pearson's correlation coefficients. Diagnostic performance was evaluated by receiver operating characteristic (ROC) curve analysis. For cell experiments, intergroup comparisons were conducted using one-way analysis of variance (ANOVA) followed by Tukey-Kramer post hoc test. A p-value <0.05 was considered statistically significant.

Results

Comparison of general data between the study and control groups

The general characteristics of all participants are presented in **Table 1**. No significant differences were observed between the groups in terms of sex, age, or BMI (all P>0.05). However,

Table 1. Comparison of general information between the study group and control group

Factor	Study group (n=96)	Control group (n=90)	χ^2/t	*P*
Gender			0.117	0.731
Male	52 (54.17)	51 (56.67)		
Female	44 (45.83)	39 (43.33)		
Age (years)	51.73±5.64	52.04±6.33	0.353	0.724
Body mass index, BMI (kg/m^2)	22.42±2.25	22.73±2.13	0.963	0.336
Type			-	-
Primary osteoporosis				
Progressive osteoporosis type I (postmenopausal osteoporosis)	41 (42.70)	-		
Progressive osteoporosis type II (senile osteoporosis)	55 (57.30)	-		
Smoking history			0.061	0.804
Yes	54 (56.25)	49 (54.44)		
No	42 (43.75)	41 (45.56)		
Drinking history			0.029	0.864
Yes	46 (47.92)	42 (46.67)		
No	50 (52.08)	48 (53.33)		
Severity				
No serious manifestation (T value <-2.5)	86 (89.58)			
Serious manifestations accompanied by fragility fracture (T value <-2.5)	10 (10.42)			
Blood calcium	2.16±0.29	2.17±0.23	0.259	0.796
Blood phosphorus	1.40±0.28	1.42±0.39	0.404	0.687
Alkaline phosphatase	213±8.13	142±6.08	67.10	<0.001
β-C-terminal telopeptide of type I collagen (β-CTX)	0.99±0.07	0.26±0.11	54.34	<0.001
Deoxypyridinoline/creatinine (DPD/Cr)	8.73±0.38	5.34±0.26	70.55	<0.001
tartrate resistant acid phosphatase 5b (TRACP-5b)	4.30±0.72	3.12±0.33	14.21	<0.001

the study group exhibited significantly higher levels of bone-specific alkaline phosphatase, β-CTX, DPD/Cr, and TRACP-5b compared to the control group (P<0.05).

Comparison of BMD before and after bisphosphonate treatment in the three subgroups

The BMD values before and after treatment for the three bisphosphonate treatment groups are shown in **Table 2**. After one year of treatment, BMD values in all three treatment groups were significantly increased compared to baseline (P<0.05).

Comparison of adverse reactions to bisphosphonate therapy and association with low miR-146a expression

In this study, adverse events were observed in 13 patients (13.5%, 13/96). Among them, 10 patients experienced mild to moderate flu-like symptoms, including fever (4 cases), fatigue (3 cases), and arthralgia/myalgia (3 cases). Additionally, 3 patients reported gastrointestinal symptoms such as nausea and vomiting. All adverse reactions resolved completely following symptomatic management. Notably, serum miR-146a levels in patients with adverse reactions were significantly lower than those in the study group (**Figure 1**, P<0.05).

MiR-146a exhibits diagnostic potential for osteoporosis

Serum miR-146a levels were significantly downregulated in the study group compared to controls (**Figure 2A**, P<0.05). ROC curve analysis demonstrated that miR-146a had strong diagnostic potential for osteoporosis, with an AUC of 0.910 (95% CI: 0.8658-0.9538), a sensitivity of 97.78%, a specificity of 77.08%, and a diagnostic threshold of 1.375 (**Figure 2B**). Furthermore, miR-146a levels were inversely correlated with osteoporosis severity, with lower expression in patients with severe disease (P<0.05) and a strong negative correlation coefficient (r=-0.615) (**Figure 2C**).

Table 2. Comparison of bone mineral density in three subgroups before and after bisphosphonate treatment

Group	Cases	Time	Lumbar vertebrae (L2-L4) ($g\text{-}cm^2$)	Neck ($g\text{-}cm^2$)	t	*P*
Risedronic acid	32	Before	0.87±0.10	0.54±0.10	13.200	<0.0001
		After	0.93±0.12	0.61±0.12	10.670	<0.0001
t			2.173	2.535	-	-
P			<0.05	<0.05	-	-
Alendronate sodium	32	Before	0.73±0.09	0.59±0.11	5.572	<0.0001
		After	0.80±0.07	0.64±0.07	9.143	<0.0001
t			3.473	2.169	-	-
P			<0.05	<0.05	-	-
Zoledronic acid	32	Before	0.74±0.06	0.63±0.13	4.346	<0.0001
		After	0.83±0.08	0.71±0.09	5.637	<0.0001
t			5.091	2.862	-	-
P			<0.05	<0.05	-	-

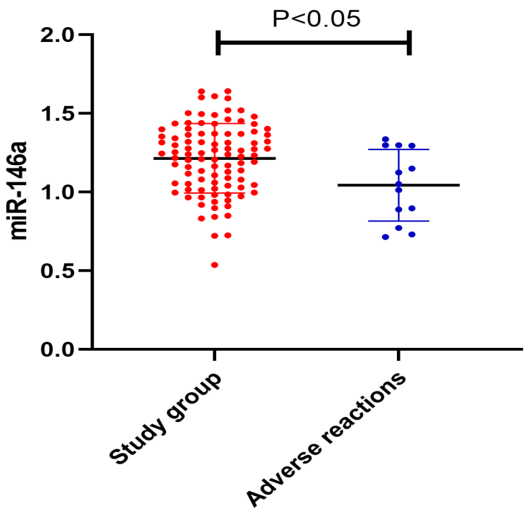

Figure 1. Low miR-146a expression is associated with adverse reactions to bisphosphonate therapies. The expression levels of miR-146a in serum samples of patients in the study group (n=96) and patients with adverse reactions (n=13) were examined using real-time quantitative reverse transcription polymerase chain reaction (RT-qPCR). The measurement data were expressed as mean ± standard deviation (SD).

MiR-146a exhibits predictive potential for efficacy of bisphosphonate therapy in osteoporosis

Serum miR-146a levels were significantly elevated after one year of bisphosphonate treatment (**Figure 3A**, P<0.05). Therapeutic outcomes were categorized as markedly effective in 27 cases, effective in 60 cases, and ineffective in 9 cases, resulting in an overall effectiveness rate of 91%. Higher post-treatment miR-146a levels were positively correlated with better therapeutic efficacy (**Figure 3B**, P<0.05). Spearman correlation analysis revealed a strong negative correlation between miR-146a expression and poor treatment outcomes (r=-0.865, P<0.05; **Figure 3C**). ROC curve analysis indicated that miR-146a had moderate predictive value for treatment efficacy, with an AUC of 0.761 (95% CI: 0.695-0.827), a sensitivity of 82.29%, a specificity of 60.42%, and a threshold of 1.280 (**Figure 3D**).

MiR-146a overexpression inhibits osteoclast differentiation

To explore the functional role of miR-146a in osteoclastogenesis, BMMCs were transfected with miR-146a mimics or inhibitors and induced to differentiate into osteoclasts. RT-qPCR confirmed that miR-146a levels were significantly increased by mimic transfection and decreased by inhibitor transfection (**Figure 4A**). TRAP staining showed that miR-146a overexpression reduced osteoclast numbers, whereas inhibition had the opposite effect (**Figure 4B**, **4C**). Western blot analysis further demonstrated that miR-146a overexpression reduced TRAP and CTSK expression levels, while inhibition increased their expression (**Figure 4D**, **4E**).

Bisphosphonates inhibit osteoclast differentiation by upregulating miR-146a expression

To elucidate the mechanism by which bisphosphonates regulate miR-146a and osteoclast

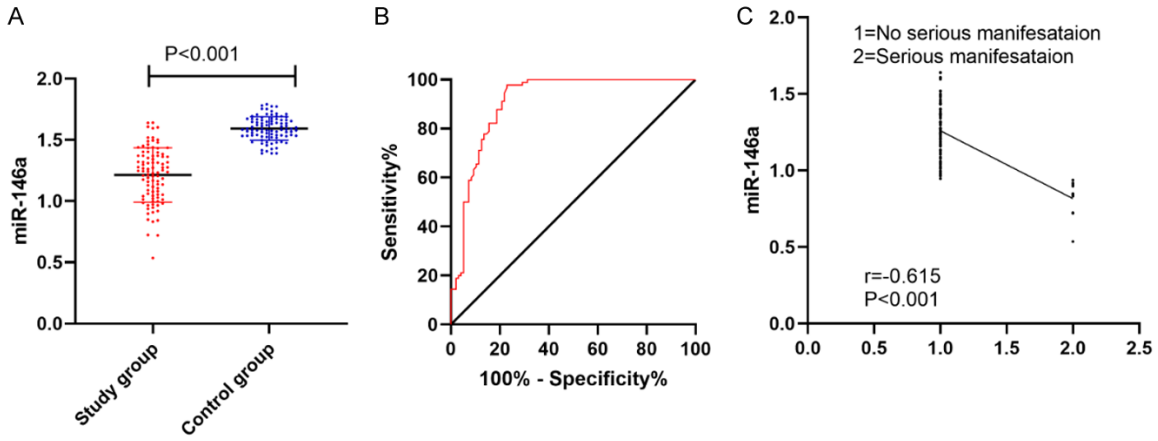

Figure 2. Diagnostic value analysis of miR-146a for osteoporosis. A: The serum miR-146a levels of patients in the study group (n=96) and control group (n=90) were examined using RT-qPCR. B: The diagnostic value of miR-146a for osteoporosis was assessed with receiver operating characteristic (ROC) curve analysis. C: The relationship between miR-146a expression and the severity of osteoporosis was evaluated with Spearman correlation analysis. No serious manifestation (n=86); Serious manifestation (n=10). The measurement data were expressed as mean ± SD.

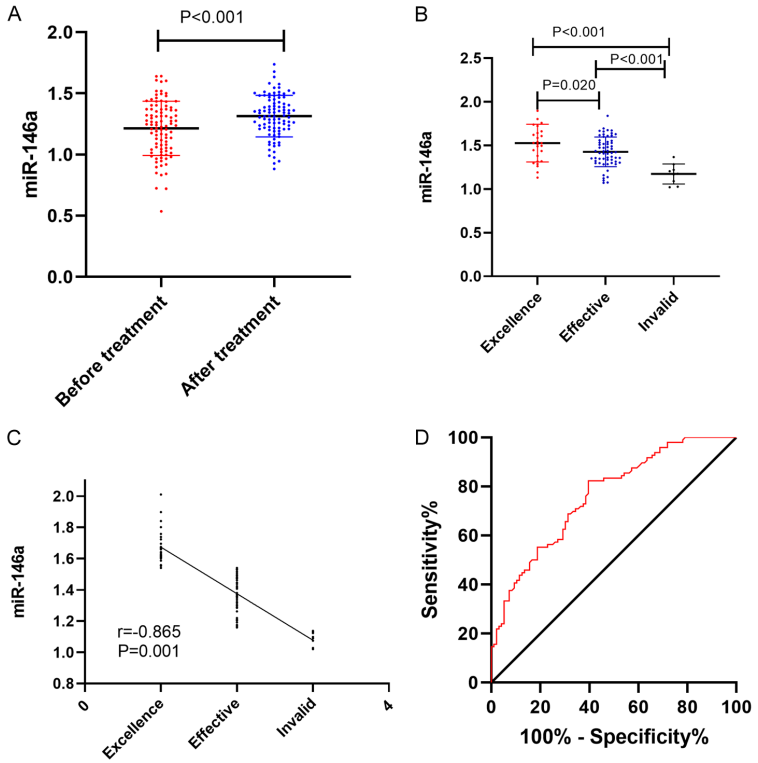

Figure 3. Evaluation of for the predicted potential of miR-146a in the efficacy of bisphosphonate therapy in osteoporosis. A: The serum miR-146a levels of osteoporosis patients in the study group (n=96) before and after treatment were examined using RT-qPCR. B: The serum miR-146a levels of patients with different therapeutic efficacies. Excellence (n=32); Effective (n=60); Invalid (n=9). C: The relationship between miR-146a expression and the therapeutic efficacies of bisphosphonate was assessed with the Spearman correlation analysis. D: The predictive value of miR-146a in osteoporosis was analyzed with the ROC curve analysis. The measurement data were expressed as mean ± SD.

differentiation, BMMCs were treated with zoledronic acid and subsequently transfected with miR-146a mimic or inhibitor. Zoledronic acid treatment significantly upregulated miR-146a expression, which was reversed by miR-146a inhibition and further enhanced by mimic transfection (**Figure 5A**). Zoledronic acid treatment reduced osteoclast numbers, an effect that was attenuated by miR-146a inhibition and amplified by miR-146a overexpression (**Figure 5B**, **5C**). Similarly, Zoledronic acid suppressed TRAP and CTSK expression; these inhibitory effects were weakened by miR-146a inhibition but strengthened by miR-146a overexpression (**Figure 5D-F**).

Discussion

Osteoporosis, a systemic metabolic bone disorder, is a major contributor to increased mortality and diminished quality of life. Recent studies report an alarming annual rise of approximately 2% in mortality

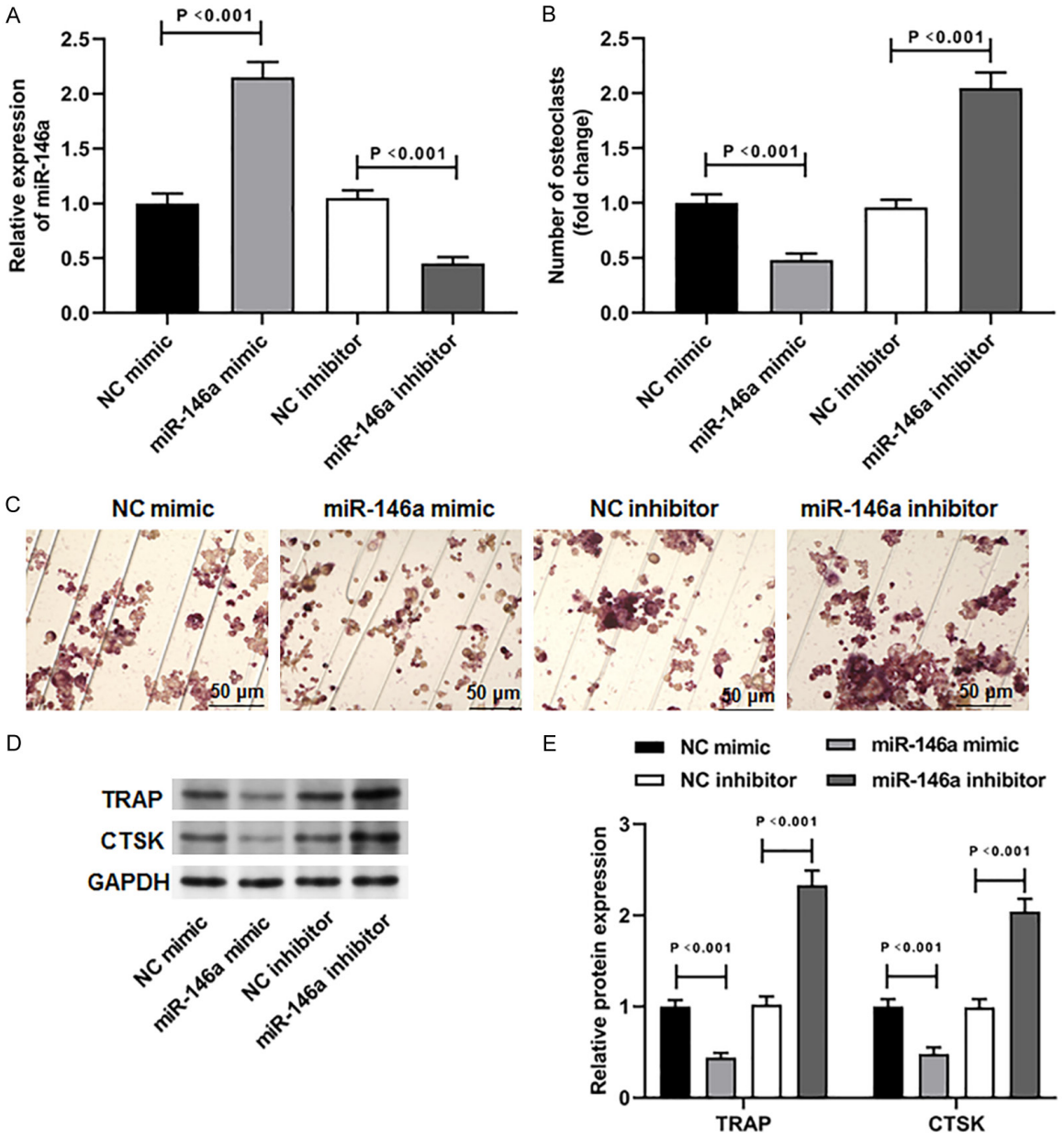

Figure 4. MiR-146a overexpression inhibits osteoclast differentiation. The isolated bone marrow mononuclear cells (BMMCs) were transfected with miR-146a mimic and inhibitor and then were induced to differentiated into osteoclasts. A: MiR-146a levels were examined by RT-qPCR; B, C: The number of osteoclasts was assessed with tartrate-resistant acid phosphatase (TRAP) strain; D, E: TRAP and cathepsin K (CTSK) protein levels were examined using Western blot analysis. N=3. The measurement data were expressed as mean ± SD.

following osteoporotic hip fractures [16]. Although BMD measurement remains fundamental to osteoporosis assessment, its clinical utility is limited by the slow rate of detectable BMD changes. Reliable evaluation of therapeutic efficacy typically requires at least annual assessments and often several years to capture significant trends [17]. These limitations highlight the urgent need for novel biological markers that can enhance diagnosis and provide more timely indicators for monitoring treatment response and disease progression.

This study primarily examined the serum expression profile of miR-146a in osteoporosis patients receiving bisphosphonate therapy and explored its potential clinical significance. The receptor activator of nuclear factor-kB (RANK)/

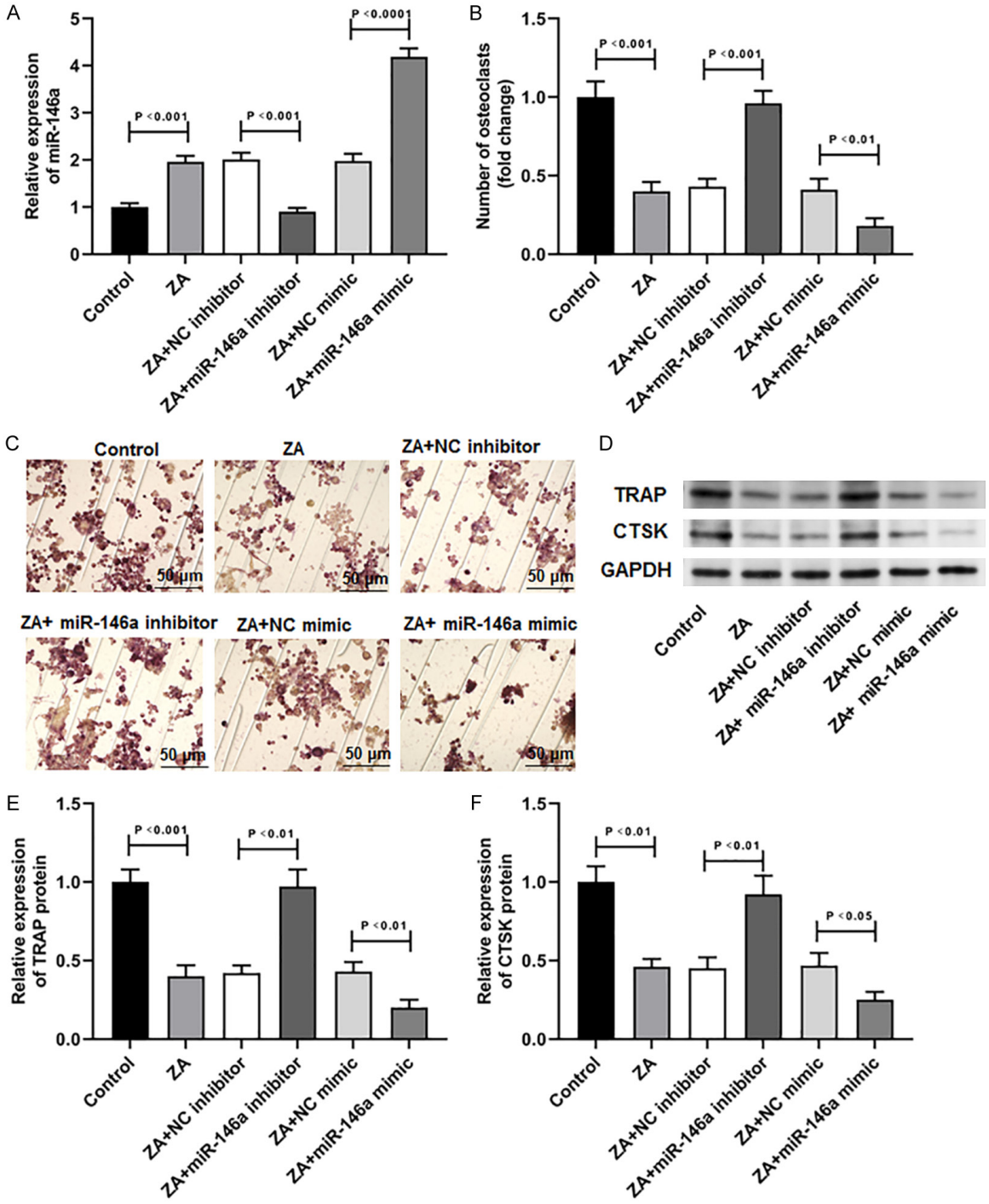

Figure 5. Bisphosphonates inhibit osteoclast differentiation by upregulating miR-146a expression. BMMCs were treated with zoledronic acid and subsequently transfected with miR-146a mimic or inhibitor. These cells were then induced to differentiate into osteoclasts. A: The level of miR-146a was examined by RT-qPCR; B, C: The number of osteoclasts was assessed using TRAP staining; D-F: TRAP and CTSK protein levels were examined with Western blot analysis. N=3. The measurement data were expressed as mean ± SD.

RANK Ligand (RANKL)/osteoprotegerin (OPG) signaling pathway is critical for osteoclast-mediated bone remodeling [18]. Emerging evidence indicates that miR-146a inhibits osteoclast differentiation induced by LPS and RANKL stimulation [19]. Animal studies have demon-

strated that zoledronic acid administration significantly reduces RANKL levels in mandibular bone tissue [20]. Furthermore, extensive research has shown that various bisphosphonates, including zoledronic acid, alendronate sodium, and chlorophosphonates, modulate osteoblast proliferation, differentiation, and the RANKL-OPG gene expression axis [21]. Collectively, these findings suggest that miR-146a may represent a promising target for bisphosphonate-based osteoporosis treatment, aligning with the primary aim of this study.

Our results showed that serum miR-146a levels were significantly downregulated in osteoporosis patients. Quantitative BMD assessments revealed no substantial differences in therapeutic outcomes among the three bisphosphonates used. Notably, after one year of bisphosphonate therapy, serum miR-146a levels were significantly elevated and negatively correlated with treatment efficacy. Moreover, serum miR-146a levels demonstrated moderate predictive value for treatment response, with an AUC of 0.761 and a sensitivity of 82.29%. These findings suggest that serum miR-146a could serve as a useful diagnostic and predictive biomarker for both osteoporosis and bisphosphonate treatment efficacy. Additionally, patients who experienced adverse reactions exhibited lower serum miR-146a levels than the overall study group, further supporting its potential as an indicator for predicting treatment-related side effects.

The underlying pathophysiology of osteoporosis involves an imbalance between bone resorption and formation, with excessive osteoclastic activity predominating. Therefore, inhibiting osteoclast differentiation is a key therapeutic strategy. Our in vitro experiments provide mechanistic insights, indicating that bisphosphonates suppress osteoclast differentiation by upregulating miR-146a expression. The combined application of bisphosphonates and miR-146a upregulation may offer a novel approach for enhancing the inhibition of bone resorption.

Recent research indicates that miR-146a plays a critical role in regulating osteoclast differentiation and is associated with disease severity [15, 22, 23]. Advances in this field have further demonstrated that miR-146a deficiency promotes osteoclast differentiation, thereby increasing bone resorption and reducing bone mass in models of inflammatory arthritis [24]. Additionally, miR-146a influences bone remodeling by modulating the differentiation of mesenchymal stem cells towards the osteogenic lineage [25]. Collectively, these findings establish miR-146a as a key regulator of bone homeostasis. Although our results suggest that bisphosphonates more effectively inhibit bone resorption when miR-146a is upregulated, the precise mechanisms underlying their combined action remain incompletely understood. To date, comprehensive analyses of the synergistic effects between miR-146a regulation and bisphosphonate therapy in osteoporosis treatment are lacking. Therefore, further validation through large-scale, multicenter studies is warranted to confirm the therapeutic potential of this combined approach.

While this study provides important insights into the role of miR-146a in osteoporosis diagnosis and bisphosphonate efficacy, several limitations should be acknowledged. First, the clinical cohort was derived from a single center with a limited sample size, which may limit the generalizability of our findings. Second, the retrospective nature of the study introduces potential selection bias and the possibility of unmeasured confounding factors, such as genetic or environmental influences. Third, although our in vitro experiments demonstrated that modulating miR-146a expression alters the effects of bisphosphonates on osteoclasts, further in vivo validation using osteoporotic animal models with genetic or pharmacological modulation of miR-146a is needed to confirm this mechanism. Fourth, it remains unclear whether the regulatory effect of miR-146a is specific to bisphosphonates or also applies to other anti-osteoporosis agents.

In summary, this study shows that miR-146a is downregulated in the serum of osteoporosis patients and upregulated after one year of bisphosphonate treatment, with its expression negatively correlated with therapeutic efficacy. Bisphosphonates inhibit osteoclast differentiation, at least in part, by upregulating miR-146a. These findings suggest that miR-146a holds promise as a diagnostic and predictive biomarker, as well as a potential therapeutic target for osteoporosis.

Disclosure of conflict of interest

None.

Address correspondence to: Haibo Yu, Department of Orthopedics, Dianjiang Traditional Chinese Medicine Hospital, No. 502 Gongnong Road, Guixi Town, Dianjiang County, Chongqing 408300, China. E-mail: 13527303837@163.com

References

[1] Johnston CB and Dagar M. Osteoporosis in older adults. Med Clin North Am 2020; 104: 873-884.

[2] Sobh MM, Abdalbary M, Elnagar S, Nagy E, Elshabrawy N, Abdelsalam M, Asadipooya K and El-Husseini A. Secondary osteoporosis and metabolic bone diseases. J Clin Med 2022; 11: 2382.

[3] Föger-Samwald U, Dovjak P, Azizi-Semrad U, Kerschan-Schindl K and Pietschmann P. Osteoporosis: pathophysiology and therapeutic options. EXCLI J 2020; 19: 1017-1037.

[4] Pang R and Xia W. Pharmacological treatment of bone loss. Curr Pharm Des 2017; 23: 6298-6301.

[5] Oryan A and Sahvieh S. Effects of bisphosphonates on osteoporosis: focus on zoledronate. Life Sci 2021; 264: 118681.

[6] Arjunan D, Bhadada T, Mohankumar SB and Bhadada SK. Non-biological antiresorptive: bisphosphonates. Indian J Orthop 2023; 57 Suppl 1: 120-126.

[7] Shetty S, John B, Mohan S and Paul TV. Vertebral fracture assessment by dual-energy X-ray absorptiometry along with bone mineral density in the evaluation of postmenopausal osteoporosis. Arch Osteoporos 2020; 15: 25.

[8] Camacho PM, Petak SM, Binkley N, Diab DL, Eldeiry LS, Farooki A, Harris ST, Hurley DL, Kelly J, Lewiecki EM, Pessah-Pollack R, McClung M, Wimalawansa SJ and Watts NB. American association of clinical endocrinologists/American college of endocrinology clinical practice guidelines for the diagnosis and treatment of postmenopausal osteoporosis-2020 update. Endocr Pract 2020; 26 Suppl 1: 1-46.

[9] Diener C, Keller A and Meese E. Emerging concepts of miRNA therapeutics: from cells to clinic. Trends Genet 2022; 38: 613-626.

[10] Iantomasi T, Romagnoli C, Palmini G, Donati S, Falsetti I, Miglietta F, Aurilia C, Marini F, Giusti F and Brandi ML. Oxidative stress and inflammation in osteoporosis: molecular mechanisms involved and the relationship with microRNAs. Int J Mol Sci 2023; 24: 3772.

[11] Mohammadisima N, Farshbaf-Khalili A and Ostadrahimi A. Up-regulation of plasma miRNA-21 and miRNA-422a in postmenopausal osteoporosis. PLoS One 2023; 18: e0287458.

[12] Ren LJ, Zhu XH, Tan JT, Lv XY and Liu Y. MiR-210 improves postmenopausal osteoporosis in ovariectomized rats through activating VEGF/Notch signaling pathway. BMC Musculoskelet Disord 2023; 24: 393.

[13] Zheng M, Tan J, Liu X, Jin F, Lai R and Wang X. miR-146a-5p targets Sirt1 to regulate bone mass. Bone Rep 2021; 14: 101013.

[14] Faraldi M, Sansoni V, Vitale J, Perego S, Gomarasca M, Verdelli C, Messina C, Sconfienza LM, Banfi G, Corbetta S and Lombardi G. Plasma microRNA signature associated with skeletal muscle wasting in post-menopausal osteoporotic women. J Cachexia Sarcopenia Muscle 2024; 15: 690-701.

[15] Minami S, Fujii Y, Yoshioka Y, Hatori A, Kaneko K, Ochiya T and Chikazu D. Extracellular vesicles from mouse bone marrow macrophages-derived osteoclasts treated with zoledronic acid contain miR-146a-5p and miR-322-3p, which inhibit osteoclast function. Bone 2025; 190: 117323.

[16] Guzon-Illescas O, Perez Fernandez E, Crespí Villarias N, Quirós Donate FJ, Peña M, Alonso-Blas C, García-Vadillo A and Mazzucchelli R. Mortality after osteoporotic hip fracture: incidence, trends, and associated factors. J Orthop Surg Res 2019; 14: 203.

[17] Lewiecki EM, Kendler DL, Davison KS, Hanley DA, Harris ST, McClung MR and Miller PD. Western osteoporosis alliance clinical practice series: treat-to-target for osteoporosis. Am J Med 2019; 132: e771-e777.

[18] De Leon-Oliva D, Barrena-Blázquez S, Jiménez-Álvarez L, Fraile-Martinez O, García-Montero C, López-González L, Torres-Carranza D, García-Puente LM, Carranza ST, Álvarez-Mon MÁ, Álvarez-Mon M, Diaz R and Ortega MA. The RANK-RANKL-OPG system: a multifaceted regulator of homeostasis, immunity, and cancer. Medicina (Kaunas) 2023; 59: 1752.

[19] Gao Y, Wang B, Shen C and Xin W. Overexpression of miR-146a blocks the effect of LPS on RANKL-induced osteoclast differentiation. Mol Med Rep 2018; 18: 5481-5488.

[20] Çankaya M, Cizmeci Şenel F, Kadioglu Duman M, Muci E, Dayisoylu EH and Balaban F. The effects of chronic zoledronate usage on the jaw and long bones evaluated using RANKL and osteoprotegerin levels in an animal model. Int J Oral Maxillofac Surg 2013; 42: 1134-1139.

[21] Elahmer NR, Wong SK, Mohamed N, Alias E, Chin KY and Muhammad N. Mechanistic insights and therapeutic strategies in osteoporosis: a comprehensive review. Biomedicines 2024; 12: 1635.

[22] Yang J, Shuai J, Siow L, Lu J, Sun M, An W, Yu M, Wang B and Chen Q. MicroRNA-146a-loaded magnesium silicate nanospheres promote bone regeneration in an inflammatory microenvironment. Bone Res 2024; 12: 2.

[23] Lin SH, Ho JC, Li SC, Chen JF, Hsiao CC and Lee CH. MiR-146a-5p expression in peripheral $CD14^+$ monocytes from patients with psoriatic arthritis induces osteoclast activation, bone resorption, and correlates with clinical response. J Clin Med 2019; 8: 110.

[24] Ammari M, Presumey J, Ponsolles C, Roussignol G, Roubert C, Escriou V, Toupet K, Mausset-Bonnefont AL, Cren M, Robin M, Georgel P, Nehmar R, Taams L, Grün J, Grützkau A, Häupl T, Pers YM, Jorgensen C, Duroux-Richard I, Courties G and Apparailly F. Delivery of miR-146a to Ly6C(high) monocytes inhibits pathogenic bone erosion in inflammatory arthritis. Theranostics 2018; 8: 5972-5985.

[25] Shen H, Jiang W, Yu Y, Feng Y, Zhang T, Liu Y, Guo L, Zhou N and Huang X. microRNA-146a mediates distraction osteogenesis via bone mesenchymal stem cell inflammatory response. Acta Histochem 2022; 124: 151913.